Journal of Hepatocellular Carcinoma

Dovepress
Taylor & Francis Group

Open Access Full Text Article

ORIGINAL RESEARCH

CT-Based Radiomics-Clinical Model for Predicting Recurrence in VETC-Positive HCC Patients After Hepatectomy

Yu Lei[1–3,*], Yaowei Bai[1–3,*], Yang Su[1–3,*], Xiatong Bai[1–3], Yingliang Wang[1–3], Chuansheng Zheng[1–3]

[1]Department of Radiology, Union Hospital, Tongji Medical College, Huazhong University of Science and Technology, Wuhan, 430022, People's Republic of China; [2]Hubei Provincial Clinical Research Center for Precision Radiology & Interventional Medicine, Wuhan, 430022, People's Republic of China; [3]Hubei Province Key Laboratory of Molecular Imaging, Wuhan, 430022, People's Republic of China

*These authors contributed equally to this work

Correspondence: Chuansheng Zheng; Yingliang Wang, Department of Radiology, Union Hospital, Tongji Medical College, Huazhong University of Science and Technology, Jiefang Avenue #1277, Wuhan, 430022, People's Republic of China, Email hqzcsxh@sina.com; 18345197920@163.com

Journal of Hepatocellular Carcinoma downloaded from https://www.dovepress.com/
For personal use only.

Objective: To construct a radiomics-based model for predicting postoperative recurrence in hepatocellular carcinoma (HCC) patients with vessels encapsulating tumor clusters (VETC) positive based on CT scan.

Methods: This retrospective study enrolled patients who underwent surgical resection between January 2016 and January 2024 at Union Hospital, with pathologic confirmation of HCC and VETC status. An external test set was drawn from Chegu Hospital, covering January 2018 to January 2022. Tumor segmentation was performed on portal venous phase CT scan, and then radiomics features were extracted. These features were further analyzed using the LASSO algorithm and combined with clinical features to construct a radiomics-clinical combination model. Model performance was evaluated using receiver operating characteristic (ROC) curves, calibration curves, and decision curve analysis (DCA). Patients were divided into high- and low-risk groups based on model scores, and Kaplan-Meier (KM) curves were compared.

Results: A total of 243 patients were included (median age 56.7 years, 211 males). Nine radiomics features and two clinical features were selected to construct the combined model. The area under the ROC curve (AUC) for predicting 1-year recurrence was 0.898 (95% CI: 0.797–0.999) in the internal test set and 0.804 (95% CI: 0.641–0.967) in the external test set. Calibration curves and DCA demonstrated high net clinical benefit of the combined model. The median recurrence-free survival (RFS) of patients in the high-risk group was significantly lower than that in the low-risk group (internal test set: 13.5 vs 30.0 months, respectively. P=0.004; external test set: 13.0 vs 31.0 months, respectively. P< 0.0001).

Conclusion: The radiomics-clinical combination model showed high accuracy for preoperatively predicting recurrence in patients with VETC-positive HCC receiving hepatectomy.

Keywords: radiomics, vessels encapsulating tumor clusters, VETC, hepatectomy, recurrence, computed tomography, hepatocellular carcinoma

Introduction

Hepatocellular carcinoma (HCC), accounting for 75–85% of primary liver cancers, is a highly aggressive malignancy with significant morbidity and mortality.[1] Its prognosis remains poor with 5-year survival rates of only 20%.[2] For early-stage patients, surgical resection is the gold standard and the most recommended treatment option, as it offers the potential for complete tumor eradication.[3] However, recurrence and metastasis, which can occur in up to 80% of cases, remain major challenges that significantly impact patient prognosis.[4]

Numerous theories have been proposed to explain the recurrence and metastasis of HCC, recent research has uncovered a novel pattern known as vessels encapsulating tumor clusters (VETC).[5] VETC is common in HCC and

Received: 26 June 2025
Accepted: 13 November 2025
Published: 19 November 2025

© 2025 Lei et al. This work is published and licensed by Dove Medical Press Limited. The full terms of this license are available at https://www.dovepress.com/terms.php and incorporate the Creative Commons Attribution – Non Commercial (unported, v4.0) License (http://creativecommons.org/licenses/by-nc/4.0/). By accessing the work you hereby accept the Terms. Non-commercial uses of the work are permitted without any further permission from Dove Medical Press Limited, provided the work is properly attributed. For permission for commercial use of this work, please see paragraphs 4.2 and 5 of our Terms (https://www.dovepress.com/terms.php).

represents an alternative pattern for HCC metastasis that is independent of epithelial-mesenchymal transition (EMT), which is one of the most widely accepted mechanisms.[6] In VETC HCC, vasculature facilitates the clumped entry of cancer cells into the bloodstream, enveloped by vascular endothelium, providing a novel and highly efficient metastatic pattern for liver cancer.[5] VETC pattern has several characteristic radiological features, including tumor size > 5.0 cm, necrosis or severe ischemia, non-smooth tumor margins, targetoid appearance, intratumoral arteries, and heterogeneous enhancement with septations or irregular ring-like structures.[7,8] Studies have indicated that HCC patients with VETC-positive have a higher recurrence rate and poorer prognosis than VETC-negative patients.[5,9–11] Ding et al discovered that VETC positive is significantly associated with micrometastatic endothelium-coated emboli and early recurrence after resection. Its poor prognosis has been confirmed in all patient subgroups stratified by tumor size, TNM classification, Barcelona Clinic Liver Cancer (BCLC) staging, and tumor invasiveness.[12] Accordingly, it is imperative to prioritize research into this distinctive vascular pattern in HCC. Especially, it is of highly significance to predict postoperative recurrence prior to hepatectomy, which can aid in personalized medical decision making.

Radiological features may correlate with the malignancy and progression rate of the tumor. Analyzing these radiological features could assist in forecasting treatment efficacy and the likelihood of postoperative recurrence. Radiomics, as an automated image analysis intelligent model, can automatically obtain innumerable quantitative features from digitally encrypted medical images.[13] Numerous radiomics-based models have already demonstrated promising performance in predicting the macrotrabecular-massive subtype, immune status, and tumor prognosis.[14,15]

Computed tomography (CT) and magnetic resonance imaging (MRI) are both standard imaging tools for patients with HCC. MRI provides excellent soft-tissue contrast, but its longer acquisition time and higher cost can limit accessibility. On contrast, CT scan offers a faster, more cost-effective, and extensively utilized imaging approach in clinical settings, with a longer-standing history in practice. In light of this, our study, for the first time, seeks to harness radiomics for the automated evaluation of tumor characteristics on CT scan among patients with VETC-positive HCC, with the goal of predicting prognosis and tumor recurrence following hepatectomy.

Materials and Methods

This study was approved by the Institutional Review Board of Union Hospital, Tongji Medical College, Huazhong University of Science and Technology and conducted in accordance with the ethical principles of the World Medical Association's Declaration of Helsinki. Since this study involves only a retrospective review of anonymized medical records without any additional intervention, and patient identities cannot be traced, written informed consent was revoked by IRB of Union Hospital, Tongji Medical College, Huazhong University of Science and Technology.

Study Design

The design flowchart of this study is shown in Figure 1. For model construction, we included a total of 182 patients who underwent hepatectomy and had histologically confirmed HCC and VETC status in Union Hospital from January 2016 to January 2024. These patients were randomly divided into a training set and an internal test set at a ratio of 7:3. For model validation, an additional 61 patients who underwent hepatectomy and had histologically confirmed HCC and VETC status from January 2018 to January 2022 at Chegu Hospital were included. The detailed inclusion and exclusion process are shown in Figure 2.

The inclusion criteria are as follows: (1) age ≥ 18 years; (2) with histological or clinical confirmation of BCLC stage A, B, or C HCC; (3) Child-Turcotte-Pugh (CTP) class A or B liver function; (4) VETC positive confirmed by CD34 immunohistochemistry; (5) underwent complete hepatectomy for HCC; (6) had baseline contrast-enhanced abdominal CT scans within 8 weeks before surgery and at least one follow-up CT scan within 6–10 weeks after surgery.

The exclusion criteria are as follows: (1) recurrent HCC or presence of other malignancies; (2) having received other treatments before surgery; (3) absence of available pathology slides for VETC evaluation; (4) CT images with artifacts or poor image quality; (5) incomplete clinical or follow-up information.

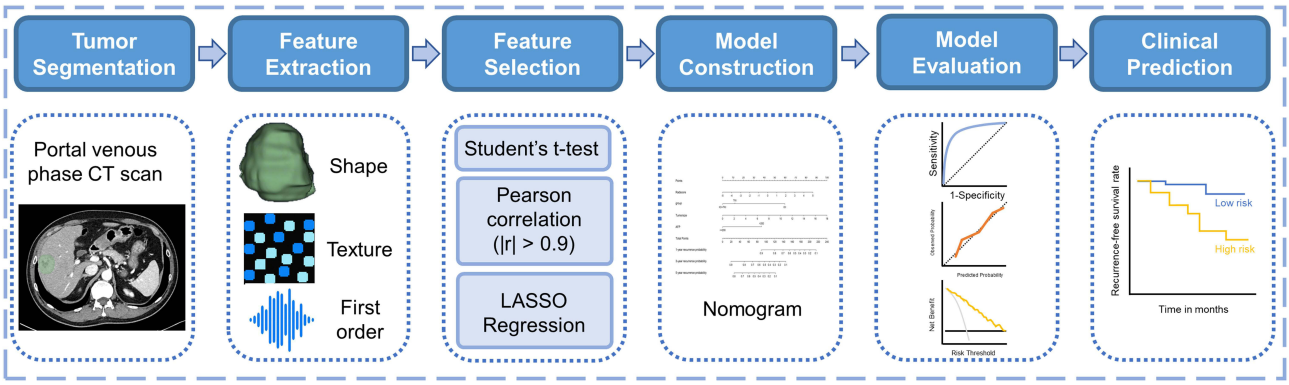

Figure 1 Design flowchart of this study. In this study, a Radiomics-clinical combination model based on the portal venous phase CT scan and clinical parameters was constructed, and their prediction performance was compared with that of radiomic and clinical models.
Abbreviations: AFP, alpha-fetoprotein; RFS, recurrence-free survival; CI, confidence interval.

Histopathology and Immunohistochemistry

The CD34 immunohistochemical staining sections of all included patients were evaluated by two experienced pathologists who were blinded to the patients' clinical and laboratory data. In case of any discrepancies, a consensus was reached through discussion. The VETC pattern is characterized by the encapsulation of individual tumor clusters by sinusoidal blood vessels, creating a network reminiscent of a cobweb.[5] VETC positive status was defined as a previous publication[16] that CD34+ vascular encapsulation occupying ≥5% of the tumor area as confirmed by CD34 immunostaining. Otherwise, it was considered VETC negative.

CT Protocols

We analyzed portal venous phase abdominal CT images of patients scanned using multi-row CT scanners from different manufacturers. Detailed imaging protocols are provided in Supplementary Materials 1: Appendix S1.

Follow-Up

Patients underwent routine follow-up with CT scan every 2–3 months within 6 months after surgery and every 3–6 months after 6 months. Tumor recurrence was defined as new intra- or extra-hepatic HCC lesions confirmed by either (1) typical enhancement pattern on contrast-enhanced CT/MRI, (2) histopathology, or (3) rising AFP after initial normalization, occurring no earlier than thirty days after curative resection. The primary endpoint is recurrence-free survival (RFS). RFS was defined as the time interval between the date of surgery and the date of recurrence or last follow-up. Follow-up was conducted until May, 2025 or until the patient's demise.

Image Segmentation and Radiomics Feature Extraction

CT scan images were extracted in Digital Imaging and Communications in Medicine (DICOM) format. Two radiologists, with 9 and 11 years of experience respectively, independently outlined the volume of interest (VOI) of the tumors on a slice-by-slice basis in the portal venous phase CT scans, utilizing the 3D Slicer software (version 5.8.0; Boston, MA, USA), without access to the patients' clinical and pathological information (Figure 3). Radiomics features extraction was performed with the PyRadiomics software (https://github.com/Radiomics/pyradiomics). In total, 1316 features were extracted for each tumor.

Clinical and Radiomics Model Development and Testing

In the training set, we analyzed the clinical parameters utilizing Cox regression analyses. Those with P value < 0.1 in the univariate analysis are further included into the multivariate analysis. The parameters ultimately selected were then incorporated into the construction of the clinical prediction model. To construct the radiomics model, the initial 1316 radiomic features were normalized with the training set's mean and standard deviation to ensure consistent scaling.

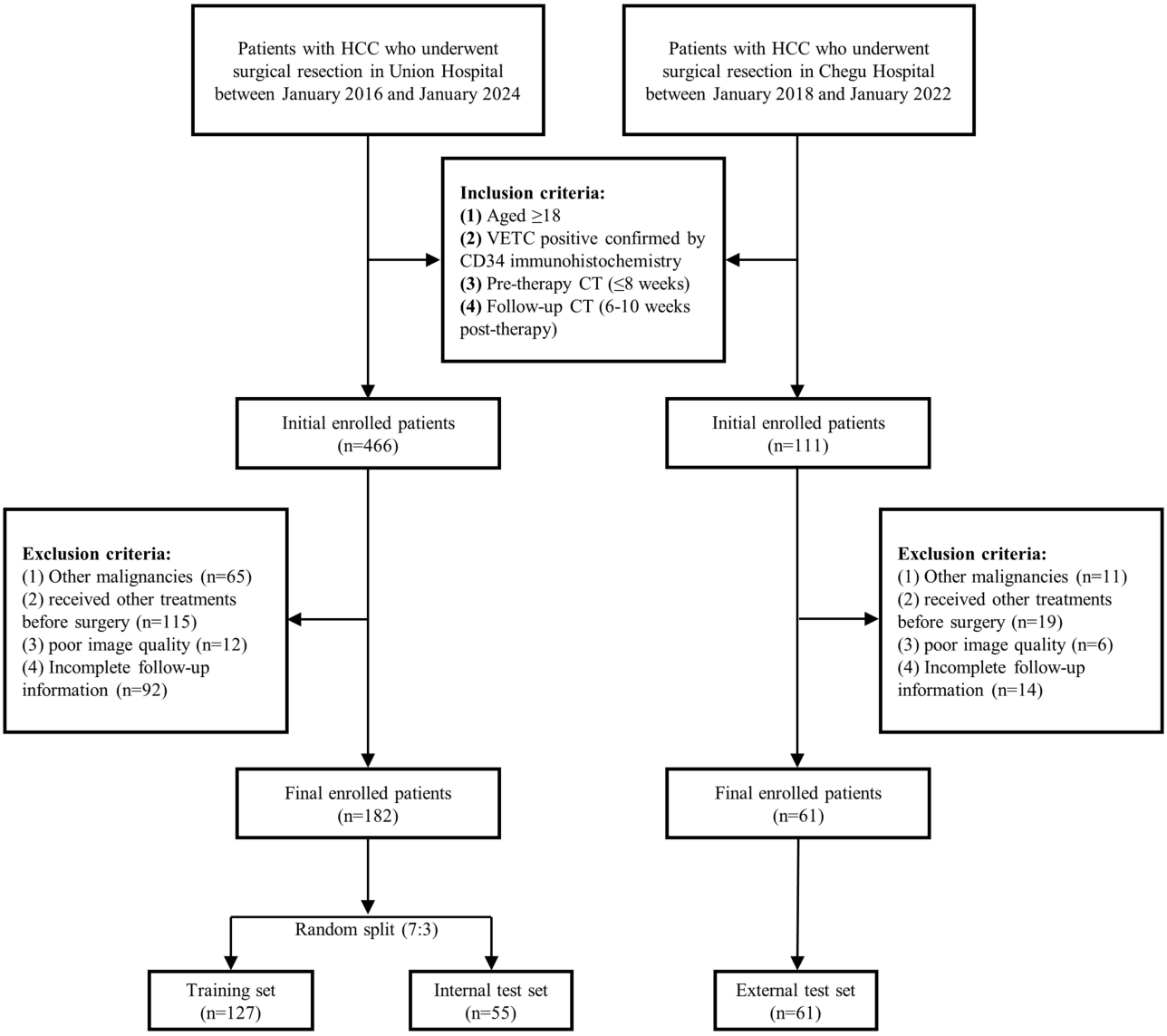

Figure 2 Patients enrollment and allocation flowchart.
Abbreviations: HCC, hepatocellular carcinoma; VETC, vessels encapsulating tumor clusters.

A *t*-test first identified features significantly associated with tumor recurrence at $p < 0.05$. Pearson correlation ($|r| > 0.9$) was then applied to discard highly correlated features and suppress multicollinearity. Finally, L1-regularized LASSO regression was applied to identify the most predictive features. The Lasso regularization parameter (λ) was determined through 10-fold cross validation. This study took λ.1se as the variable screening criterion. The final selected features were subsequently incorporated into the development of the radiomics model. Besides, we constructed a radiomics-clinical combined model by integrating the clinical parameters from the clinical model and the Radscore derived from the radiomics model, which is a score calculated by integrating all radiomics parameters.

Nomograms were created for three models. Receiver operating characteristic (ROC) curves and calibration curves were used to evaluate model performance, while decision curve analysis (DCA) was utilized to assess the clinical value. Besides, patients were stratified into high-risk and low-risk categories using the optimal cutoff value obtained from the nomogram of the combined model in training set, which was determined by the surv_cutpoint function from the "survminer" R package. Kaplan–Meier (KM) survival curves were plotted to compare the prognosis between the two groups.

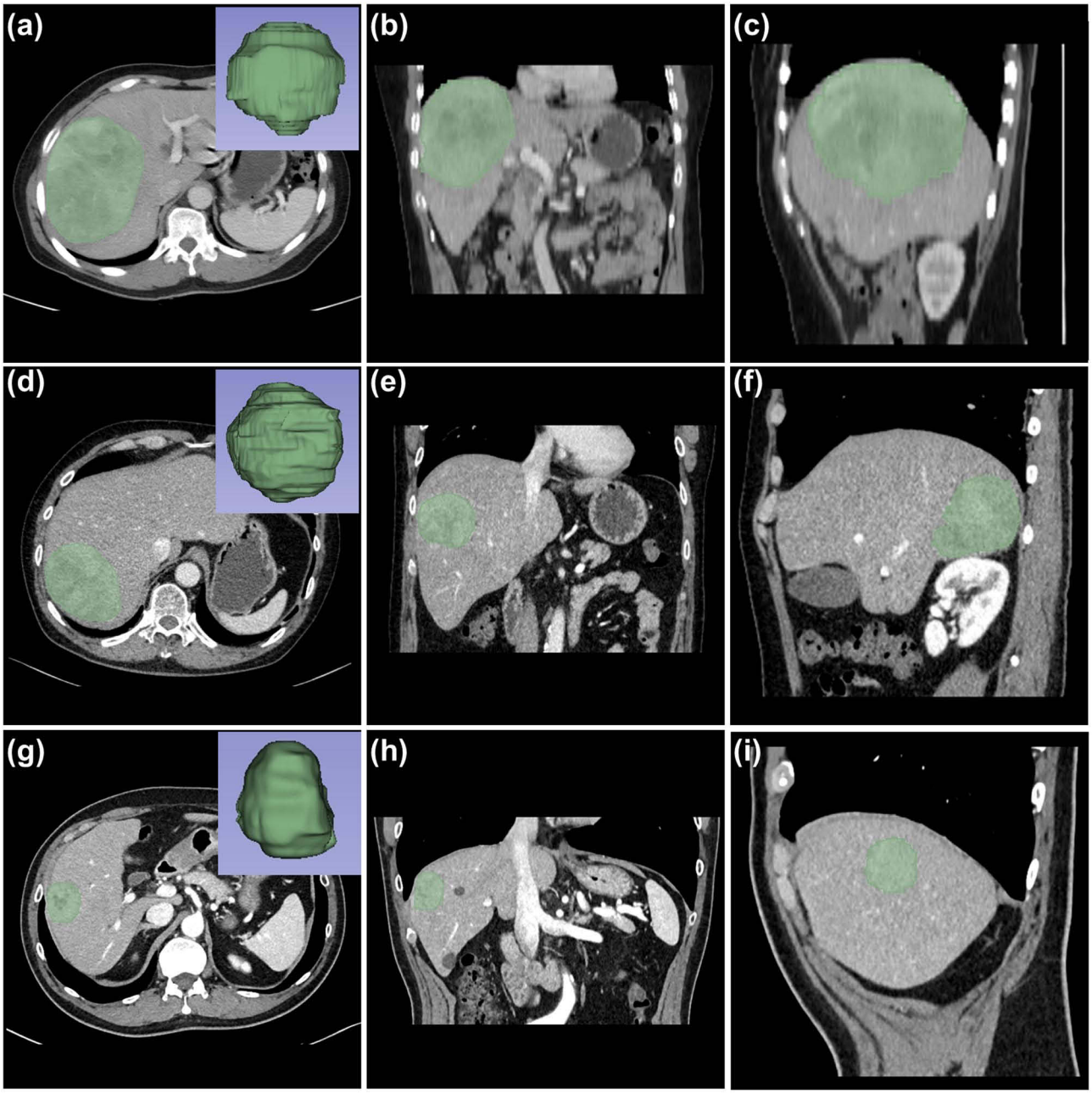

Figure 3 CT images and segmentations in three patients. (**a–c**), (**d–f**), and (**g–i**) show the transverse, coronal, and sagittal CT images of the abdomen for Patient 1, 2, and 3, respectively, together with their corresponding volume-rendered images; the tumors are highlighted in green.

Statistical Analysis

Descriptive statistics are used to summarize patient characteristics and their laboratory values, presented as numbers (percentages) or mean ± standard deviation (SD). The Student's *t*-test is used for continuous variables, and the Wilcoxon rank-sum test is used for variables that did not meet the criteria for normal distribution or for ordered variables. The chi-square test or Fisher's exact test are applied to compare group differences. Kaplan–Meier survival curves and Log rank tests are conducted using the "survival" and "survminer" R packages to illustrate the survival differences between the two groups. Uni- and multivariable Cox regression analyses were performed to identify potential independent prognostic factors of RFS. The DeLong test was employed to compare the ROC curves. Calibration was evaluated using the Hosmer–Lemeshow goodness-of-fit test, where $P > 0.05$ indicates adequate calibration. A p-value < 0.05 was considered

statistically significant for all analyses. Statistical analysis was conducted using Python version 3.10 and R version 4.4.2 (https://www.r-project.org).

Results

Patients Characteristics

The characteristics of the patients in the training set, internal test set, and external test set are summarized in Table 1. The median ages of the patients in the training set, internal test set, and external test set were 56.54 ± 11.59, 55.02 ± 11.45, and 58.66 ± 11.79, respectively. The proportions of male patients were 87.4%, 85.5%, and 86.9%, respectively. Most patients were classified as CTP class A and had BCLC stage A. The prevalence of hepatitis B virus (HBV) infection was 75.6%, 74.5%, and 75.4%, respectively. The median tumor sizes were 5.99 ± 2.98 cm, 6.59 ± 3.46 cm, and 5.58 ± 2.55 cm, respectively. There were no significant differences in the baseline characteristics of the patients across the three datasets.

Table 1 Baseline Characteristics of Patients

	All (n=243)	Training Set (n=127)	Internal Test Set (n=55)	External Test Set (n=61)	P value
Sex, n (%)					0.938
Female	32 (13.2)	16 (12.6)	8 (14.5)	8 (13.1)	
Male	211 (86.8)	111 (87.4)	47 (85.5)	53 (86.9)	
Age, y	56.72 (11.63)	56.54 (11.59)	55.02 (11.45)	58.66 (11.79)	0.235
CTP class, n (%)					0.872
A	191 (78.6)	100 (78.7)	42 (76.4)	49 (80.3)	
B	52 (21.4)	27 (21.3)	13 (23.6)	12 (19.7)	
BCLC stage, n (%)					0.926
A	164 (67.5)	86 (67.7)	35 (63.6)	43 (70.5)	
B	26 (10.7)	14 (11.0)	7 (12.7)	5 (8.2)	
C	53 (21.8)	27 (21.3)	13 (23.6)	13 (21.3)	
Tumor number					0.968
1	201 (82.7)	105 (82.7)	45 (81.8)	51 (83.6)	
>1	42 (17.3)	22 (17.3)	10 (18.2)	10 (16.4)	
Hypertension					0.574
No	170 (70.0)	89 (70.1)	41 (74.5)	40 (65.6)	
Yes	73 (30.0)	38 (29.9)	14 (25.5)	21 (34.4)	
Diabetes					0.921
No	203 (83.5)	107 (84.3)	45 (81.8)	51 (83.6)	
Yes	40 (16.5)	20 (15.7)	10 (18.2)	10 (16.4)	
Hepatitis B virus					0.989
No	60 (24.7)	31 (24.4)	14 (25.5)	15 (24.6)	
Yes	183 (75.3)	96 (75.6)	41 (74.5)	46 (75.4)	
Cirrhosis					0.277
No	101 (41.6)	53 (41.7)	27 (49.1)	21 (34.4)	
Yes	142 (58.4)	74 (58.3)	28 (50.9)	40 (65.6)	
Portal hypertension					0.418
No	151 (62.1)	78 (61.4)	38 (69.1)	35 (57.4)	
Yes	92 (37.9)	49 (38.6)	17 (30.9)	26 (42.6)	
Radscore	0.44 (1.67)	0.45 (1.66)	0.61 (1.28)	0.27 (1.99)	0.563
Tumor size, cm	6.03 (3.00)	5.99 (2.98)	6.59 (3.46)	5.58 (2.55)	0.193
Laboratory parameters					
PT, s	13.89 (1.23)	13.88 (1.23)	14.00 (1.39)	13.81 (1.09)	0.695
INR	1.10 (0.15)	1.10 (0.15)	1.11 (0.14)	1.10 (0.16)	0.968
TBIL, μmol/L	1.26 (2.08)	1.28 (2.12)	1.16 (1.00)	1.30 (2.67)	0.924

(*Continued*)

Table 1 (Continued).

	All (n=243)	Training Set (n=127)	Internal Test Set (n=55)	External Test Set (n=61)	P value
ALB, g/L	38.02 (5.52)	38.14 (5.52)	37.95 (5.78)	37.84 (5.34)	0.939
ALT, U/L	57.41 (117.23)	56.46 (115.19)	72.07 (160.08)	46.15 (64.60)	0.491
AST, U/L	68.79 (135.55)	67.20 (133.10)	95.36 (185.38)	48.13 (69.91)	0.170
ALP, U/L	112.72 (157.86)	111.50 (155.17)	102.93 (70.66)	124.08 (212.69)	0.767
TBA, μmol/L	16.39 (28.85)	16.34 (28.58)	13.51 (23.46)	19.24 (33.85)	0.575
TP, g/L	64.19 (6.12)	64.37 (6.28)	62.93 (6.20)	64.97 (5.62)	0.185
Cr, μmol/L	0.79 (0.18)	0.80 (0.21)	0.77 (0.15)	0.81 (0.15)	0.608
UA, μmol/L	313.15 (98.55)	314.06 (97.87)	317.60 (105.15)	307.16 (95.06)	0.843
AFP					0.842
≤200 ng/mL	166 (68.3)	87 (68.5)	36 (65.5)	43 (70.5)	
>200 ng/mL	77 (31.7)	40 (31.5)	19 (34.5)	18 (29.5)	
RBC, ×10^12/L	4.31 (0.66)	4.31 (0.66)	4.37 (0.69)	4.23 (0.64)	0.543
WBC, ×10^9/L	5.11 (2.22)	5.12 (2.18)	5.32 (2.40)	4.90 (2.14)	0.591
Plt, ×10^9/L	156.05 (66.73)	157.69 (66.89)	161.96 (71.04)	147.30 (62.50)	0.460
Hb, g/L	130.92 (18.50)	131.10 (18.30)	131.55 (19.47)	129.98 (18.30)	0.892
Neutrophils, ×10^9/L	4.85 (1.11)	4.77 (1.05)	5.05 (1.87)	3.01 (1.84)	0.488
Lymphocyte, ×10^9/L	1.35 (0.52)	1.35 (0.52)	1.36 (0.55)	1.32 (0.51)	0.878
NLR	4.16 (11.73)	4.09 (11.51)	5.97 (17.23)	2.66 (2.16)	0.316

Note: Values are presented as means ± SD and n (%).

Abbreviations: CTP, Child-Turcotte-Pugh score; BCLC, Barcelona Clinic Liver Cancer staging system; PT, prothrombin time; INR, international normalized ratio; TBIL, total bilirubin; ALB, albumin; ALT, alanine aminotransferase; AST, aspartate aminotransferase; ALP, alkaline phosphatase; TBA, total bile acid; TP, total protein; Cr, creatinine; UA, uric acid; AFP, alpha-fetoprotein; RBC, red blood cell count; WBC, white blood cell count; Plt, platelet count; Hb, hemoglobin; NLR, neutrophil-to-lymphocyte ratio.

Radiomics Features and Clinical Characteristics Selection

Among the 1316 radiomic features, the LASSO method ultimately identified nine significant parameters for constructing the radiomics model (Supplementary Figure 1). The specific parameters are as follows: "square_gldm_DependenceVariance", "gradient_glszm_LowGrayLevelZoneEmphasis", "gradient_glszm_SmallAreaLowGrayLevelEmphasis", "logarithm _glszm_ZoneVariance", "logarithm_glszm_LargeAreaEmphasis", "wavelet. HLL_ngldm_Busyness", "original_shape_ Flatness", "wavelet.HHH_glszm_GrayLevelNonUniformityNormalized", "wavelet. LHL_glcm.ldmn" (see Supplementary Materials: Supplementary Figure 1). The nomogram derived from the radiomics model is shown in Figure 4A.

Multivariate Cox regression analysis ultimately identified two parameters: tumor size and alpha-fetoprotein (AFP) (Table 2). Clinical model was constructed based on these parameters. The nomogram derived from the clinical model is shown in Figure 4B.

Furthermore, a combined model was constructed by incorporating the Radscore from the radiomics model with the clinical parameters from the clinical model. The nomogram derived from the combined model is shown in Figure 4C.

Predictive Value of Combined Model for Postoperative Recurrence

The median follow-up time was 19 months (IQR: 8.0–31.5 months). In the training set, 74 of the 127 patients experienced tumor recurrence, with a median RFS of 15.0 months. In the internal test set, 32 of the 55 patients experienced tumor recurrence, with a median RFS of 15.0 months. In the external test set, 35 of 61 patients experienced tumor recurrence, with a median RFS of 16.0 months. The AUC for predicting 1-year recurrence of the combined model was 0.843 (95% CI: 0.745–0.940) in the training set, 0.898 (95% CI: 0.797–0.999) in the internal test set, and 0.804 (95% CI: 0.641–0.967) in the external test set (Figure 5A–C). In the training set, the combined model achieved an accuracy of 0.885, sensitivity of 0.835, and specificity of 0.956. In the internal test set, it achieved an accuracy, sensitivity, and specificity of 0.917, 0.882, and 0.966, respectively. In the external test set, performance remained robust, with an accuracy of 0.809, a sensitivity of 0.799, and a specificity of 0.823 (Table 3). Calibration curves of the combination

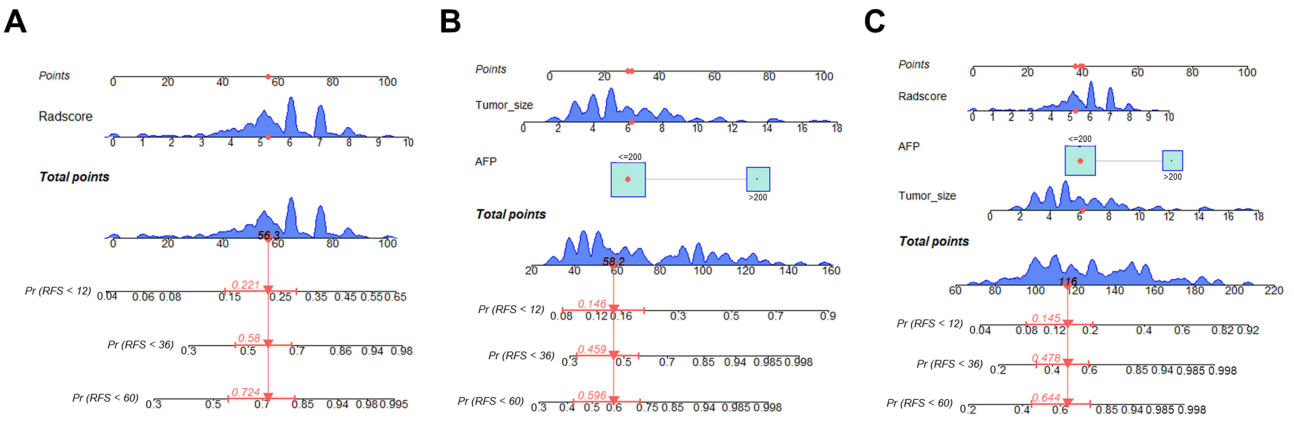

Figure 4 Nomograms of radiomics (**A**), clinical (**B**) and combination models (**C**) for predicting postoperative recurrence in hepatocellular carcinoma patients.
Abbreviations: Rad_Score, radiomics prediction score; AFP, alpha-fetoprotein; RFS, recurrence-free survival.

model for predicting 1-year recurrence closely aligned the predicted and observed outcomes across the three datasets (P > 0.05; Figure 5D–F). Furthermore, DCA across the three datasets demonstrated that the combination model provides higher clinical net benefit compared to both the treat-all and treat-none strategies for predicting 1-year (Figure 5G–I) recurrence.

Table 2 Uni- and Multivariable Analyses of Factors Associated with Recurrence

Factor	Univariable Analysis			Multivariable Analysis		
	HR	95% CI	*P* value	HR	95% CI	*P* value
Sex (Male vs Female)	0.54	0.29–1.02	0.059	1.04	0.50–2.14	0.920
Age, y	1.00	0.98–1.02	0.928			
CTP class (B vs A)	0.74	0.42–1.31	0.307			
BCLC stage						
B vs A	1.21	0.54–2.68	0.648			
C vs A	1.37	0.81–2.32	0.242			
Tumor number (>1 vs 1)	1.25	0.68–2.29	0.472			
Hypertension (yes vs no)	0.69	0.41–1.18	0.177			
Diabetes (yes vs no)	1.24	0.70–2.19	0.459			
Hepatitis B virus (yes vs no)	1.07	0.62–1.85	0.816			
Cirrhosis (yes vs no)	0.87	0.54–1.40	0.568			
Portal hypertension (yes vs no)	1.66	1.04–2.66	0.035	1.54	0.90–2.62	0.112
Radscore	1.39	1.17–1.66	<0.001	1.23	1.03–1.47	0.023
Tumor size, cm	1.16	1.09–1.24	<0.001	1.13	1.04–1.21	0.003
Laboratory parameters						
PT, s	1.05	0.84–1.32	0.649			
INR	1.86	0.27–13.03	0.530			
TBIL, μmol/L	1.00	1.00–1.01	0.288			
ALB, g/L	1.05	1.01–1.09	0.026	1.03	0.99–1.06	0.167
ALT, U/L	1.00	1.00–1.00	0.002	1.00	1.00–1.00	0.060
AST, U/L	1.00	1.00–1.00	0.163			
ALP, U/L	1.00	1.00–1.00	0.617			
TBA, μmol/L	1.00	1.00–1.01	0.459			
TP, g/L	1.01	0.97–1.05	0.679			
Cr, μmol/L	0.99	0.98–1.01	0.262			
UA, μmol/L	1.00	1.00–1.00	0.283			

(*Continued*)

Table 2 (Continued).

Factor	Univariable Analysis			Multivariable Analysis		
	HR	95% CI	*P* value	HR	95% CI	*P* value
RBC, ×10^12/L	1.19	0.83–1.71	0.336			
WBC, ×10^9/L	0.99	0.89–1.10	0.881			
Plt, ×10^9/L	1.00	1.00–1.00	0.483			
Hb, g/L	1.01	0.99–1.02	0.301			
Neutrophils, ×10^9/L	0.98	0.93–1.04	0.602			
Lymphocyte, ×10^9/L	1.00	0.63–1.60	0.999			
NLR	1.00	0.98–1.02	0.946			
AFP (>200 ng/mL vs ≤200 ng/mL)	3.19	1.97–5.16	<0.001	2.36	1.37–4.09	0.002

Note: Variables with univariable p< 0.1 were introduced in multivariable analysis.
Abbreviations: HR, hazard ratio; CI, confidence interval; CTP, Child-Turcotte-Pugh score; BCLC, Barcelona Clinic Liver Cancer staging system; PT, prothrombin time; INR, international normalized ratio; TBIL, total bilirubin; ALB, albumin; ALT, alanine aminotransferase; AST, aspartate aminotransferase; ALP, alkaline phosphatase; TBA, total bile acid; TP, total protein; Cr, creatinine; UA, uric acid; RBC, red blood cell count; WBC, white blood cell count; Plt, platelet count; Hb, hemoglobin; NLR, neutrophil-to-lymphocyte ratio; AFP, alpha-fetoprotein.

Moreover, the combined model also demonstrated excellent performance in predicting 3- and 5-year tumor recurrence, with ROC curves, calibration plots, and DCA curves presented in Supplementary Figures 2–4.

Performance Comparison Between Models

Overall, the combined model demonstrated superior discrimination performance in predicting post-operative recurrence of VETC-positive HCC compared with either the clinical model or the radiomics model alone (Figure 5). As shown in Tables 3 and 4, combined model achieved higher AUCs compared to clinical model in the training set (combined vs clinical: 0.843 vs 0.618, P < 0.001), the internal test set (0.898 vs 0.731, P = 0.127), and the external test set (0.804 vs 0.478, P = 0.005). Although the differences did not reach statistical significance, combined model consistently delivered numerically superior metrics relative to the radiomics model across all datasets: 0.843 vs 0.830 (P = 0.564) in the training set, 0.898 vs 0.881 (P = 0.480) in the internal test set, and 0.804 vs 0.732 (P = 0.109) in the external test set.

Risk Stratification

In the training set, the combined model achieved an AUC of 0.843 for distinguishing high- and low-risk groups for tumor recurrence after hepatectomy, with an optimal cutoff value of 90.2. This cutoff was then applied to three datasets to classify patients into high- and low-risk groups for recurrence. In the training set, KM curves showed that the median RFS was 13.0 months for the high-risk group and 30.0 months for the low-risk group, with a significant difference between the two groups (P < 0.0001) (Figure 6A). Similarly, KM curves showed that the median RFS of the high-risk group was significantly shorter than that of the low-risk group in test set (internal test set: 13.5 vs 30.0 months, respectively; P=0.004; external test set: 13.0 vs 31.0 months, respectively; P < 0.0001) (Figure 6B and C).

Discussion

HCC with the VETC pattern is a highly aggressive subtype that is associated with a high recurrence rate and poor prognosis following hepatectomy.[5,10] Due to its unique vascular structure, the sinusoidal network of functional blood vessels in VETC can release entire tumor clusters into the bloodstream through open vessels, thereby facilitating tumor metastasis.[5,17] Therefore, it is crucial to accurately predict postoperative recurrence in these patients for better clinical decision making. To our knowledge, there has been no research in this topic to date. This study is the first to develop and validate a radiomics-clinical combination model based on CT scan. The model integrates both radiomics features extracted from CT scan and clinical parameters, achieving high AUC in the training set, internal test set, and external test set. Calibration curves have proven the predictive accuracy of the model, and DCA has demonstrated the clinical significance of the model. These results significantly outperform both the radiomics model and the clinical model alone.

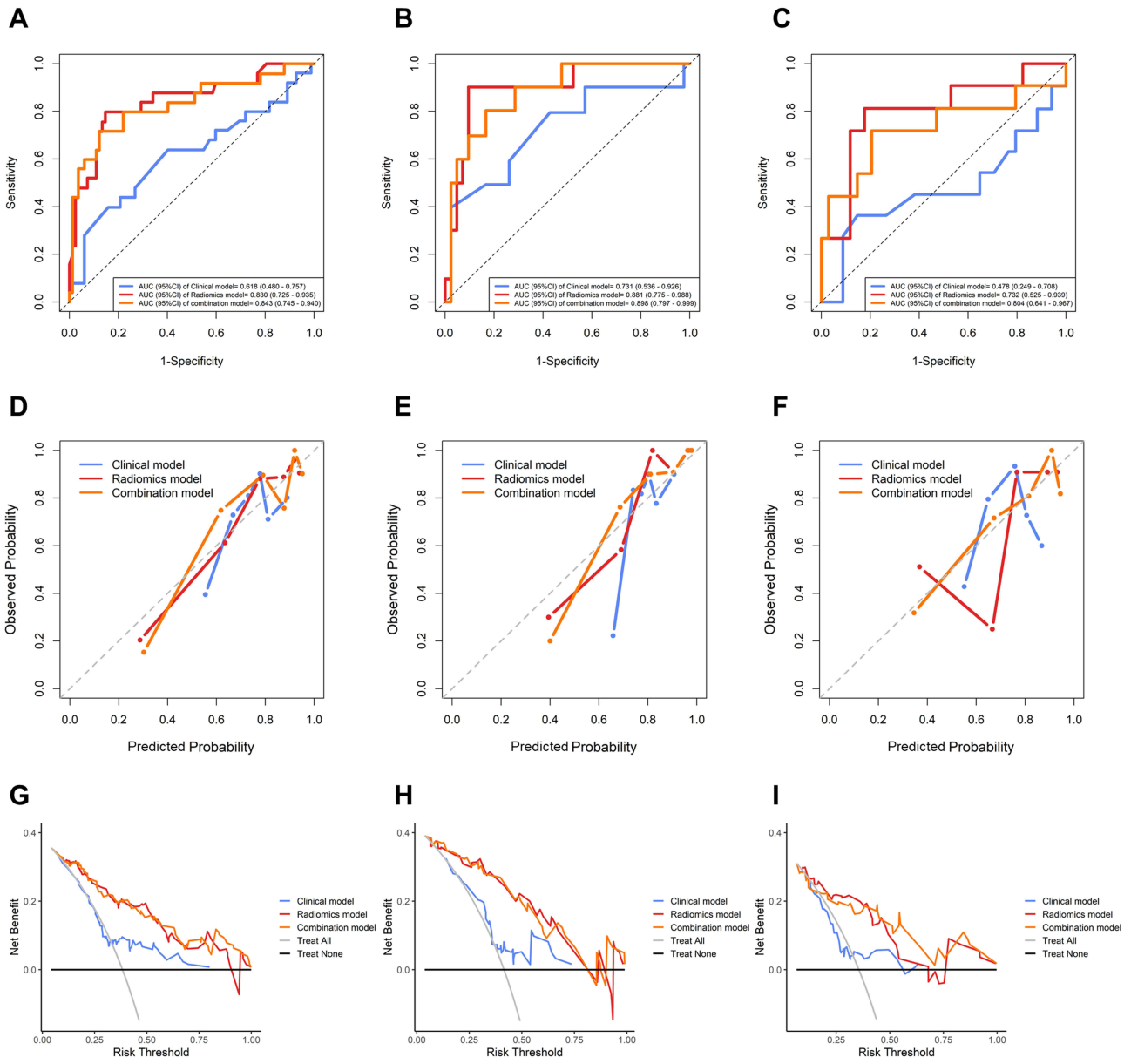

Figure 5 Performance of three models for predicting postoperative recurrence at 1 year. (**A–C**) Receiver operating characteristic (ROC) curve analysis for the training set (**A**), internal test set (**B**) and external test set (**C**). **(D–F)** Calibration curves for the training set (**D**), internal test set (**E**) and external test set (**F**). (**G–I**) Decision curve analysis (DCA) curves for the training set (**G**), internal test set (**H**) and external test set (**I**).
Abbreviation: AUC, area under the ROC curve.

Additionally, the combined model is capable of assessing the likelihood of postoperative recurrence in patients prior to surgery, thereby categorizing them into high-risk and low-risk groups. KM curves show that the recurrence-free survival time of the high-risk group is significantly lower than that of the low-risk group.

The radiomics model identified nine significant features from the portal venous phase CT scan, encompassing both shape and texture characteristics. The feature "original_shape_Flatness" measures the flatness of the tumor, particularly its degree of irregularity. Tumors with higher flatness may have more irregular edges, potentially invading surrounding tissues more readily and thus increasing the risk of recurrence.[7,18] The remaining eight texture features reflect the spatial distribution, size, and gradient changes of different gray-level regions within the tumor.[19] Low gray-level areas may correspond to necrotic or ischemic regions within the tumor,[18] and their spatial distribution and size are closely related to the tumor's malignancy. In VETC-positive hepatocellular carcinoma (HCC), tumor clusters encapsulated by endothelial

Table 3 Results of Models' Predictive Ability for Recurrence at 1 Year

Models	Dataset	AUC (95% CI)	Acc	Sen	Spe	PPV	NPV	F1
Clinical	Train	0.618 (0.480–0.757)	0.657	0.609	0.724	0.755	0.570	0.674
	Internal test	0.731 (0.536–0.926)	0.722	0.673	0.789	0.816	0.634	0.738
	External test	0.478 (0.249–0.708)	0.484	0.408	0.587	0.571	0.424	0.476
Radiomics	Train	0.830 (0.725–0.935)	0.864	0.821	0.924	0.938	0.787	0.876
	Internal test	0.881 (0.775–0.988)	0.882	0.864	0.907	0.928	0.827	0.895
	External test	0.732 (0.525–0.939)	0.749	0.724	0.783	0.818	0.678	0.768
Combined	Train	0.843 (0.745–0.940)	0.885	0.835	0.956	0.964	0.806	0.895
	Internal test	0.898 (0.797–0.999)	0.917	0.882	0.966	0.973	0.855	0.925
	External test	0.804 (0.641–0.967)	0.809	0.799	0.823	0.859	0.753	0.828

Abbreviations: Acc, accuracy; Sen, sensitivity; Spe, specificity; PPV, positive predictive value; NPV, negative predictive value.

Table 4 DeLong's Test for ROC Curves Comparison of Clinical Model, Radiomics Model and Combined Model

Compared Groups	Training Set	Internal Test Set	External Test Set
	P value	P value	P value
Combined vs Clinical	<0.001	0.127	0.005
Combined vs Radiomics	0.564	0.480	0.109

cells often experience compromised blood flow. The constrictive effect of endothelial wrapping, combined with outward pressure from proliferating tumor cells, can narrow the vascular lumen, leading to reduced oxygen and nutrient supply and the formation of localized ischemic regions. Meanwhile, continued tumor expansion increases the distance from existing vasculature, further exacerbating hypoxia. This rapid growth, accompanied by ongoing yet insufficient neovascularization, creates a cycle of intermittent hypoxia and ultimately results in prominent necrosis.[20] Consequently, a large number of low-gray-level regions implies that highly proliferative tumor cells are more likely to breach the endothelial sleeve surrounding the tumor cluster, facilitating dissemination and metastasis and subsequently increasing the risk of

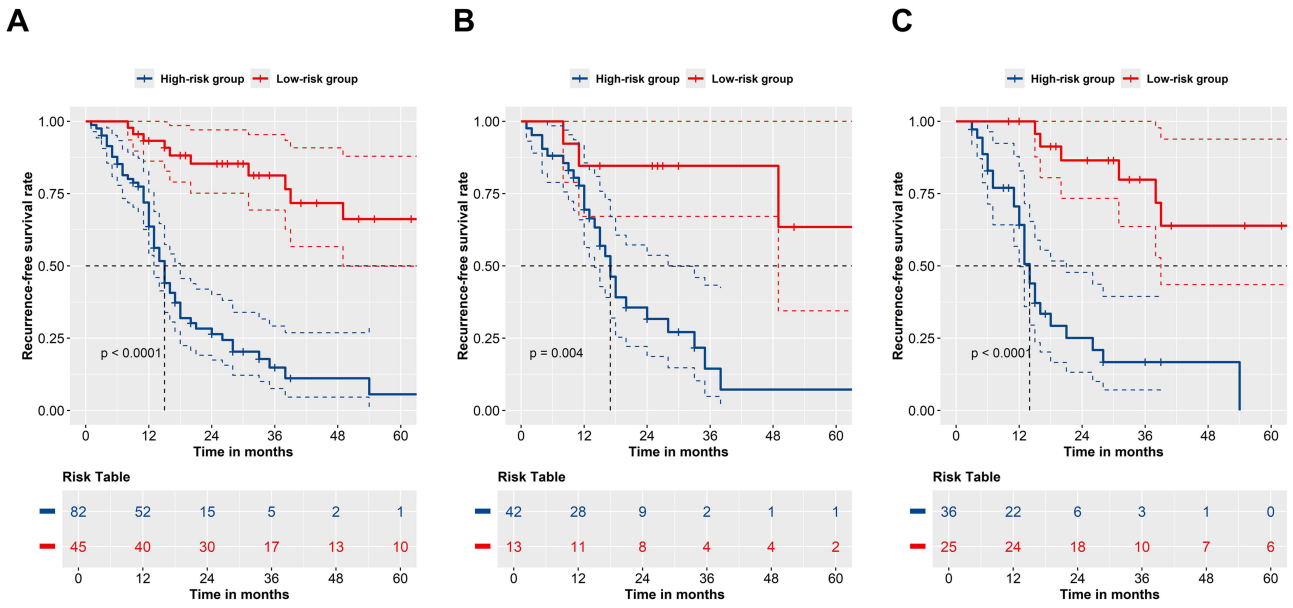

Figure 6 Kaplan-Meier analysis for predicting postoperative recurrence in high and low-risk patients on the training set (**A**), internal test set (**B**), and external test set (**C**).

https://doi.org/10.2147/JHC.S549825

post-operative recurrence. Higher gradient changes in gray-level values reflect the identical pathobiology: high-density viable tissue interdigitates with low-density necrotic areas, indicating more complex internal tumor structures with abundant edges and textural variations. These features, which are characteristic of biologically aggressive neoplasia, confer an amplified probability of intravascular invasion and early postoperative relapse.[21–23]

The clinical model included two parameters: tumor size and AFP level. Tumor size has long been recognized as a critical prognostic indicator in HCC. VETC-positive tumors tend to be larger, typically exceeding 5 cm in maximum diameter.[8] Extensive research has consistently demonstrated that larger tumors are correlated with an increased likelihood of tumor recurrence.[7] This relationship underscores the importance of tumor size in predicting disease progression and recurrence. AFP serves as a valuable biomarker in the context of HCC, providing insights into the tumor's burden and its potential for aggressive behavior.[24] Generally speaking, elevated AFP levels are indicative of more advanced stages of the tumor and are associated with a higher risk of disease progression and metastases,[25] which is consistent with our findings.

Several studies have delved into the application of radiomics for predicting outcomes in HCC, yet few have concentrated specifically on the VETC-positive subtype. The VETC-positive pattern, as a unique vascular type, accounts for 30 to 40 percentage of HCC patients and is characterized by a higher metastatic potential and poorer prognosis.[9] Our study bridges this gap by illustrating the viability and efficacy of utilizing radiomics to analyze the distinctive CT features linked to VETC. By identifying individuals with a heightened risk of postoperative recurrence, clinicians can consider implementing more aggressive supplementary treatments or initiating more frequent monitoring protocols.

However, our study has several limitations. Firstly, as the study was conducted at a single center, the findings might be influenced by the specific patient demographic, types of CT machines, and scanning methodologies employed. Multi-center studies would be beneficial to confirm the model's applicability in diverse clinical settings. Secondly, our study did not integrate pathological imaging or incorporate radiopathomics, which could potentially enhance the model's predictive power. Lastly, our model was not developed using deep learning methods, which have shown promise in recent studies for improving diagnostic and prognostic accuracy. Future research should explore the integration of pathological imaging and the application of deep learning techniques to further refine and enhance the predictive capabilities of our model.

In summary, our radiomics-clinical combination model presents an innovative and potent method for forecasting postoperative recurrence in VETC-positive HCC patients. By integrating radiomics features and clinical parameters, the model offers high accuracy and clinical utility. Subsequent research endeavors should aim to tackle the limitations highlighted and validate the model in multi-center prospective studies to augment its performance further.

Data Sharing Statement

The data of this study are available from the corresponding author (Chuansheng Zheng and Yingliang Wang) on reasonable request.

Ethical Statements

This study was approved by the Institutional Review Board of Union Hospital, Tongji Medical College, Huazhong University of Science and Technology and conducted in accordance with the ethical principles of the World Medical Association's Declaration of Helsinki. Since this study involves only a retrospective review of anonymized medical records without any additional intervention, and patient identities cannot be traced, written informed consent was revoked by IRB of Union Hospital, Tongji Medical College, Huazhong University of Science and Technology.

Acknowledgments

We would like to express my sincere thanks to all members of our research team for their invaluable contributions to this study.

Author Contributions

All authors made a significant contribution to the work reported, whether that is in the conception, study design, execution, acquisition of data, analysis and interpretation, or in all these areas; took part in drafting, revising or critically

reviewing the article; gave final approval of the version to be published; have agreed on the journal to which the article has been submitted; and agree to be accountable for all aspects of the work.

Funding

This study was supported by National Natural Science Foundation of China (82402406, U22A20352) and National Key R&D Program of China (2023YFC2413500).

Disclosure

The authors declare that they have no known competing financial interests or personal relationships that could have appeared to influence the work reported in this paper.

References

1. Xie D, Shi J, Zhou J, Fan J, Gao Q. Clinical practice guidelines and real-life practice in hepatocellular carcinoma: a Chinese perspective. *Clin Mol Hepatol*. 2023;29:206–216. doi:10.3350/cmh.2022.0402
2. Siegel RL, Miller KD, Fuchs HE, Jemal A. Cancer statistics, 2022. *CA Cancer J Clin*. 2022;72:7–33. doi:10.3322/caac.21708
3. Reig M, Forner A, Rimola J, et al. BCLC strategy for prognosis prediction and treatment recommendation: the 2022 update. *J Hepatol*. 2022;76:681–693. doi:10.1016/j.jhep.2021.11.018
4. Vogel A, Meyer T, Sapisochin G, Salem R, Saborowski A. Hepatocellular carcinoma. *Lancet*. 2022;400:1345–1362. doi:10.1016/S0140-6736(22)01200-4
5. Fang JH, Zhou HC, Zhang C, et al. A novel vascular pattern promotes metastasis of hepatocellular carcinoma in an epithelial-mesenchymal transition-independent manner. *Hepatology*. 2015;62:452–465. doi:10.1002/hep.27760
6. Giannelli G, Koudelkova P, Dituri F, Mikulits W. Role of epithelial to mesenchymal transition in hepatocellular carcinoma. *J Hepatol*. 2016;65:798–808. doi:10.1016/j.jhep.2016.05.007
7. Feng Z, Li H, Zhao H, et al. Preoperative CT for characterization of aggressive macrotrabecular-massive subtype and vessels that encapsulate tumor clusters pattern in hepatocellular carcinoma. *Radiology*. 2021;300:219–229. doi:10.1148/radiol.2021203614
8. Pan J, Huang H, Zhang S, et al. Intraindividual comparison of CT and MRI for predicting vessels encapsulating tumor clusters in hepatocellular carcinoma. *Eur Radiol*. 2025;35:61–72. doi:10.1007/s00330-024-10944-9
9. Liu K, Dennis C, Prince DS, et al. Vessels that encapsulate tumour clusters vascular pattern in hepatocellular carcinoma. *JHEP Rep*. 2023;5:100792. doi:10.1016/j.jhepr.2023.100792
10. Renne SL, Woo HY, Allegra S, et al. Vessels Encapsulating Tumor Clusters (VETC) is a powerful predictor of aggressive hepatocellular carcinoma. *Hepatology*. 2020;71:183–195. doi:10.1002/hep.30814
11. Zhang P, Ono A, Fujii Y, et al. The presence of vessels encapsulating tumor clusters is associated with an immunosuppressive tumor microenvironment in hepatocellular carcinoma. *Int, J, Cancer*. 2022;151:2278–2290. doi:10.1002/ijc.34247
12. Ding T, Xu J, Zhang Y, et al. Endothelium-coated tumor clusters are associated with poor prognosis and micrometastasis of hepatocellular carcinoma after resection. *Cancer*. 2011;117:4878–4889. doi:10.1002/cncr.26137
13. Gillies RJ, Kinahan PE, Hricak H. Radiomics: images are more than pictures, they are data. *Radiology*. 2016;278:563–577. doi:10.1148/radiol.2015151169
14. Feng Z, Li H, Liu Q, et al. CT radiomics to predict macrotrabecular-massive subtype and immune status in hepatocellular carcinoma. *Radiology*. 2023;307:e221291. doi:10.1148/radiol.221291
15. Zhong ME, Duan X, Ni-Jia-Ti MY, et al. CT-based radiogenomic analysis dissects intratumor heterogeneity and predicts prognosis of colorectal cancer: a multi-institutional retrospective study. *J Transl Med*. 2022;20:574. doi:10.1186/s12967-022-03788-8
16. Lin W, Lu L, Zheng R, et al. Vessels encapsulating tumor clusters: a novel efficacy predictor of hepatic arterial infusion chemotherapy in unresectable hepatocellular carcinoma. *J Cancer Res Clin Oncol*. 2023;149:17231–17239. doi:10.1007/s00432-023-05444-0
17. Kawasaki J, Toshima T, Yoshizumi T, et al. Prognostic impact of Vessels that Encapsulate Tumor Cluster (VETC) in patients who underwent liver transplantation for hepatocellular carcinoma. *Ann Surg Oncol*. 2021;28:8186–8195. doi:10.1245/s10434-021-10209-5
18. Chen FM, Du M, Qi X, et al. Nomogram estimating vessels encapsulating tumor clusters in hepatocellular carcinoma from preoperative gadoxetate disodium-enhanced MRI. *J Magn Reson Imaging*. 2023;57:1893–1905. doi:10.1002/jmri.28488
19. Brenet Defour L, Mulé S, Tenenhaus A, et al. Hepatocellular carcinoma: CT texture analysis as a predictor of survival after surgical resection. *Eur Radiol*. 2019;29:1231–1239. doi:10.1007/s00330-018-5679-5
20. Tohme S, Yazdani HO, Liu Y, et al. Hypoxia mediates mitochondrial biogenesis in hepatocellular carcinoma to promote tumor growth through HMGB1 and TLR9 interaction. *Hepatology*. 2017;66:182–197. doi:10.1002/hep.29184
21. Matsuda K, Ueno A, Tsuzaki J, et al. Vessels encapsulating tumor clusters contribute to the intratumor heterogeneity of HCC on Gd-EOB-DTPA-enhanced MRI. *Hepatol Commun*. 2025;9:e0593. doi:10.1097/HC9.0000000000000593
22. Feng ST, Jia Y, Liao B, et al. Preoperative prediction of microvascular invasion in hepatocellular cancer: a radiomics model using Gd-EOB-DTPA-enhanced MRI. *Eur Radiol*. 2019;29:4648–4659. doi:10.1007/s00330-018-5935-8
23. Yu Y, Fan Y, Wang X, et al. Gd-EOB-DTPA-enhanced MRI radiomics to predict vessels encapsulating tumor clusters (VETC) and patient prognosis in hepatocellular carcinoma. *Eur Radiol*. 2022;32:959–970. doi:10.1007/s00330-021-08250-9
24. Fan Y, Xue H, Zheng H. Systemic therapy for hepatocellular carcinoma: current updates and outlook. *J Hepatocell Carcinoma*. 2022;9:233–263. doi:10.2147/JHC.S358082
25. Tzartzeva K, Obi J, Rich NE, et al. Surveillance imaging and alpha fetoprotein for early detection of hepatocellular carcinoma in patients with cirrhosis: a meta-analysis. *Gastroenterology*. 2018;154:1706–18.e1. doi:10.1053/j.gastro.2018.01.064

Journal of Hepatocellular Carcinoma

Dovepress
Taylor & Francis Group

Publish your work in this journal

The Journal of Hepatocellular Carcinoma is an international, peer-reviewed, open access journal that offers a platform for the dissemination and study of clinical, translational and basic research findings in this rapidly developing field. Development in areas including, but not limited to, epidemiology, vaccination, hepatitis therapy, pathology and molecular tumor classification and prognostication are all considered for publication. The manuscript management system is completely online and includes a very quick and fair peer-review system, which is all easy to use. Visit http://www.dovepress.com/testimonials.php to read real quotes from published authors.

Submit your manuscript here: https://www.dovepress.com/journal-of-hepatocellular-carcinoma-journal